Failure modes and shear design of prestressed hollow core slabs made of fiber-reinforced concrete

E. Cuenca[1]; P. Serna[2]

Institute of Concrete Science and Technology (ICITECH), Universitat Politècnica de València, Camí de Vera s/n, 46022 Valencia, Spain[1, 2]

escueas@upvnet.upv.es[1], pserna@cst.upv.es[2]

Abstract

Hollow core slabs (HCS) are usually precast by extrusion and it is not easy to place stirrups; thus, it is difficult to guarantee shear resistance in some cases. This paper describes an experience using fiber-reinforced concrete (FRC) to produce HCS by extrusion to gain shear reinforcement.

An experimental program consisting of 26 HCS was developed. Elements were produced and tested in shear according to the following variables: amount of steel fibers (0, 50 and 70 kg/m^3) and a shear span/depth (a/d) ratio of 2.3 to 4.4 and 8.6.

Different failure modes took place. Some of the main conclusions drawn were that fibers act as shear reinforcement, HCS with fibers achieved greater loads than HCS without fiber reinforcement and with a more ductile behavior.

Keywords

A. Fibres; B. Strength; D. Mechanical testing; E. Extrusion.

1. Introduction

Hollow core slabs (HCS) were developed in the 1950s when long-line prestressing techniques evolved [1]. HCS are advanced products in the prestressed precast concrete industry, especially in terms of efficient use of material (low self-weight), and given their high quality due to the efficient production line manufacturing process [2, 3]. The extrusion method has a very widespread use and has been utilized to produce inexpensive and easy-to-handle HCS [2, 4-11]. Nevertheless, the extrusion method is not without its drawbacks because it does not allow shear reinforcement incorporation, and anchorage reinforcement by bond is produced. Shear on HCS and its failure modes have been studied by different authors [1-14],

who analyzed various failure modes: flexure, anchorage and shear (by web shear tension or by shear-flexure).

The parameters which mainly affect the shear strength of prestressed precast HCS are amount of prestress force, concrete strength (compressive and tensile strengths), loading conditions, and interlocking forces in the shear crack.

Given the circumstances, introducing fibers into concrete could improve the shear capacity [15-17] of the HCS. Paine et al. [8-11, 14] experimentally studied shear on HCS made with fiber-reinforced concrete (FRC), using 48kg/m^3 of hooked-end steel fibers, 30 mm in length, with an aspect ratio of 60 by testing them with an a/d of 2, 3 and 4.5. The conclusions they drew were: manufacture of extruded HCS reinforced with steel fibers has been shown to be practicable; addition of steel fibers to HCS increases the first crack and ultimate shear capacity; the nature of improvement was dependent on the a/d ratio; the post-cracking ductility of fiber-reinforced slabs also substantially improved in comparison with plain slabs; a safer, controlled failure was observed.

Nowadays, the relevant method to calculate HCS is given in European Standard EN 1168+A2 [18]. This Standard deals with the requirements and the basic performance criteria and specifies minimum values where appropriate for precast hollow core slabs made of prestressed or reinforced normal weight concrete according to EN 1992-1-1:2004. This European Standard covers terminology, performance criteria, tolerances, relevant physical properties, special test methods, and special aspects of transport and erection. However, it is not contemplated the contribution of steel fibers to the HCS resistance, in those cases MC2010 [19, 20] and RILEM [21] approach will be used to determine the contribution of steel fibers to shear resistance.

2. Research significance

Given the impossibility of placing stirrups in the HCS produced by extrusion, introduction of steel fibers into concrete can prove to be a system that helps improve shear resistance. However, the literature includes very few works on the shear behavior of HCS made with FRC and does not offer characterization tests in relation to HCS made with FRC which can be adapted to Current Design Codes.

In this paper, introduction of FRC as shear reinforcement in a continuous way has been conducted in a precast plant where 26 real-scale HCS were produced. The extrusion process was carried out with

concretes with several amounts of steel fibers: 0, 50 and 70kg/m^3. Hence, the shear behavior of HCS produced with two prestressing levels and different amounts of steel fibers has been studied.

3. Experimental investigation

Twenty-six HCS were tested and classified into two different series, mainly differenced by the tension in the prestressing strands and the different design failure modes expected in them.

In Series I, HCS and their test disposition were designed so that failures were produced by shear-flexure. For Series II, a program with greater variability of predictable failure modes was developed, and was based on a design for more heavily prestressed HCS which contemplates a wider range of fiber reinforcement amounts.

3.1. Hollow core slabs' geometry.

All the HCS presented the same geometry (Figure 1) and a depth of 260mm. This geometry is within the scope of application of the European Standard EN 1168+A2 [18]. A different reinforcement disposition, characterized by the number and diameter of wire or strand, its position and tension applied (Figure 1 and Table 1), was tested in each Series. In Table 1, "*Initial tensile*" is the prestressing tension applied prior to discounting prestressing losses; r_{inf} is the cover on the bottom of HCS; ρ_l is the reinforcement ratio for longitudinal reinforcement (wires or 7-wire strands in this case) and σ_c is the average stress acting on the concrete cross-section for an axial force due to prestressing actions. Series I and II adopted the HCS notations used in the precast industry: PF 26.20 and PF 26.16, respectively.

As Table 1 shows, Series I (PF26.20) included wires (Y 1860 C 5.0) with a diameter of 5mm and 7-wire strands (Y 1860 S7 9.3), thus conforming a strand with a nominal diameter equal to 9.3mm (the notation is defined in UNE 36094-97 and EN 10027-1) with a yielding stress f_{pk} equal to 1637MPa and, a tensile strength of 1860MPa for the wires, and yielding stress f_{pk} equal to 1581MPa and a tensile strength of 1860MPa for strands. In Series II (PF26.16), on the other hand, only those wires with the same characteristics as those in Series I were used. All these values were nominal.

3.2. Concrete mix design.

One important goal was to produce HCS by extrusion with very dry concretes by adding different amounts of steel fibers (0, 50 and 70kg/m^3). To carry out the desired objective, several mix designs were employed.

The materials used in this study were a CEM I 52.5R cement type and calcareous crushed aggregates: 0/4mm-sized sand, 0/6mm-sized sand and 6/10mm-sized gravel. The steel fibers utilized were low carbon steel with hooked-end (RC 65/40 BN), 40mm in length, 0.62mm in diameter, with an aspect ratio (length/diameter) equal to 65.

Two concrete admixtures were used: an accelerating high range water reducer/superplasticizer and a specific admixture for extruded concretes.

Table 2 presents the mix designs.

The concrete without fibers was used in the daily HCS production in the collaborating precast industry. Mechanical properties were controlled in one concrete sample by means of the compressive strength test on 150 x 300 mm cylinders (EN 12390-3) and the flexural tensile strength test (EN 14651). The following were obtained with the flexural test: the residual flexural tensile strength ($f_{R,j}$), which corresponds to the crack mouth opening displacements (CMOD) linked to the crack openings of 0.5, 1.5, 2.5 and 3.5mm (j=1,2,3,4 respectively).

Table 3 provides the mechanical properties of the different concrete mixes. All the values were obtained as an average of three specimens made with two different samples for each concrete type 28 days after casting HCS.

3.3. HCS production.

A continuous slab was casted. It occupied a complete lane in which prestressed strands were positioned; the machine received the concrete and HCS were formed by extrusion (Figure 2).

As expected [14], some problems initially occurred when a new concrete type was produced. The initial problems were related with introducing fibers into a very dry concrete mix to obtain an optimum concrete ready to use in the extrusion process. Yet after the preliminary adjustments in the process, these problems no longer appeared and a good surface aspect was achieved (Figure 3). This fact demonstrates that it is possible to produce HCS with FRC in a normal daily production cycle in a precast plant.

Only some slabs had undulations on their surface, webs of different widths and defects on the slab surface, which were created in some zones where fibers blocked the extrusion machine.

3.4. Test set-up.

HCS were subjected to a four-point test according to the disposition shown in Figure 4. Figure 5 depicts the test set-up. Tests were done in the precast industry.

Loads and supports were disposed into two cross lines. The shear span/depth (a/d) ratio varied between 3 and 4.4 in Series I. In Series II, there were three different a/d ratios: 2.3, 3.4 and 8.6. Table 4 indicates all these parameters. In order to facilitate their identification and ulterior analysis, the HCS Specimen ID took the following structure:

{Series: I or II} - {Amount of fibers (kg/m^3)} - {a/d ratio} {a, b, c, ...}

If there were identical HCS, they were differentiated by placing: a, b, c, etc. So, an HCS from Series II with 50kg/m^3 of fibers, and with a/d=3.4, which had other identical HCS, would be: II-50-3.4b.

In order to analyze the previous precrack effect, three HCS (14, 18 and 24) were precracked before the shear test by loading the HCS with a longer span length (a/d=4.9) since the maximum flexure crack width reached was 0.2mm. In these precrack steps, a shear of 161kN was accomplished.

After the flexure precracking tests, supports were moved to adapt them to shear tests conditions so that shear failure was on the flexure precracked zone.

Table 4 shows not only the variables analyzed for each test, but also the maximum load reached and the main failure mode. Figure 6 indicates the evaluated section for web shear tension failures which, in this case, had been adopted as the intersection between the centroidal axis of the HCS and the failure line that emerges from the edge of the support with an angle of 35 ° to the horizontal axis, as indicated EN 1168+A2 [18], which delimitates the zone affected by the support reaction.

Several HCS were tested with a critical length (l_{crit}) below the transfer length (l_{pt}), which was evaluated according to the European standard EN 1168+A2 [18] which, in this aspect, refers to the standard EN 1992-1-1 [22]. In some HCSs, this caused anchorage failure (HCS 4, 12 and 22). Nevertheless HCS 9, which was also performed with a critical length below the transfer length failure, there was no anchorage failure; the reason was that the crack which caused the failure was at a long distance from the cantilever. The values are presented in Table 4.

4. Tests results and analysis

4.1. Failure modes.

Different failure modes were observed. The following notation was used:

-SHEAR FAILURE MODES:

-SF: Shear-flexure failure, Fig.7.

On the shear-flexure failures, flexure cracks initially developed, but eventually one of them caused the failure. The failure crack was always situated in the shear span close to one of the load points. Firstly, the crack grew vertically to finally turn in direction by taking a shear slope near the top.

-*S: Web shear tension failure of concrete; Fig. 5.*

In most cases, failure was caused by diagonal shear tension. Shear failure was produced by inclined cracks due to principal tensile stresses. On these slabs, a transverse reinforcement was not placed to resist shear, so fibers, prestressing strands and the concrete zone in compression had to resist shear solicitations; if shear grew, the crack progressed upwardly to the HCS top.

-FLEXURE MODE (Fig.8):

-*F: Flexure failure.*

For the greatest a/d ratio in Series II (a/d=8.6), several flexure cracks developed vertically toward the top of the HCS, and one of these cracks continued to grow until a flexure failure took place.

-FAILURE ON ANCHORAGE OF PRESTRESSING STRANDS:

-*A: Anchorage failure of strands; Fig.9.*

During the tests, slippage on strands was also detected and, in most cases, this led to a diagonal crack.

4.2. Load-Deflection Response.

Figure 10 plots the deflections on the mid-span for the most representative HCS of Series I.

As expected, HCS 4 failed through anchorage and the failure was brittle. All the other HCS failed through shear-flexure and showed a ductile failure. The maximum load increased when shear span diminished. HCS with fibers exhibited greater shear capacities.

In Figures 11-a, 11-b and 11-c, the load-deflections curves of Series II are plotted and classified by fibers amount according to the shear span (a/d) ratio. Three behaviors are distinguished. HCS with a/d=2.3 accomplished the greatest loads with brittle failure through a diagonal shear (S).

In these cases, and especially when the critical length l_{crit} was close to the transfer length l_t (II-0-2.3 and II-70-2.3b), final failure was caused by anchorage. For HCS II-70-2.3a, the main failure was caused by web shear tension failure (S), but it seems clear that the contribution of prestressing was weak. Signs of this were reflected by the low loads reached and the embrittlement observed after the peak. In this case, the l_{crit} was only a few millimeters above l_{pt}.

The lowest ultimate loads corresponded to the HCS with a/d=8.6. In this supports-loads distribution, the highest deflections were achieved, showing clear ductile failure by flexure (F) or shear-flexure (SF). In these cases, behavior was similar for the three types of concrete as the influence of fibers was only marginal compared with the influence of the prestress.

The HCS with an *a/d* ratio=3.4 showed intermediate behavior by always cracking through web shear tension failure (S). The tendency of increasing shear capacity with an increasing amount of fibers is reported.

For the a/d =3.4 ratio, we can see (Fig 11-d) that the HCS, which previously cracked in flexure (HCS 14, 18 and 24), accomplished a more ductile behavior with greater loads than their equivalent non precracked HCS. Moreover, dependence on fiber amount was clearly evident.

4.3. Shear values according to current Design Codes and failure modes discussion.

Some authors like Pisanty [7] and Bertagnoli [12], among others, claimed that the model proposed in EC2 [22] to evaluate the uncracked shear capacity of prestressed elements overestimated the real ultimate strength. For this reason, the standard EN 1168+A2 [18] proposes a reduction of shear resistance proposed by the EC2 [22]. Therefore, the shear capacity by diagonal shear tension was calculated assuming the region as uncracked in bending using the formula (1) of EN 1168+A2 [18], as this standard has no formulation to take into account fiber contribution, henceforth it will be calculated by following the RILEM formula [21]; the values are indicated in Table 5 (see Notation from Appendix A). The safety margins (SM) were obtained as V_{test} / V_{theo} (the shear test value divided by the shear theoretical value).

$$V_{Rdc}=\varphi\cdot (I\cdot b/S)\cdot\sqrt{(f_{ct}^{2}+\beta\cdot\alpha_l\cdot\sigma_{cd}\cdot f_{ct})} \quad (1)$$

Shear strength capacities were calculated by the formulation of standard EN 1168+A2 [18] under cracked conditions (*based on EC2 [22]*) adding fibers contribution (*RILEM [21]*), and MC2010 [19, 20]. To obtain the elements' shear theoretical values, each HCS can be approximated to a single double T beam; so web width b_o was the sum of all the webs widths which composed the HCS. For the calculations, the fact that all the webs contributed in the same manner to resist shear was taken into account. However, some authors, like Elliott [10], suggested that the shear capacity of HCS was not the same as the shear capacity of each component section, unless web widths were all exactly equal; thus, shear failure finally occurred in the critical web. Therefore, it was reasonable to calculate shear by not taking into account all the webs composing HCS. As HCS were treated as a sum of the double T beams, the contribution of the flange to the shear was considered in the calculations for the HCS made from fibers by means of factor k_f

(Appendix B), present in the RILEM formula. This value (k_f) was equal to 1.036 for all the cases. Neither EN 1168+A2 nor MC2010 considered flanges contribution to shear. For the HCS made without fibers, MC2010 shear strength was calculated by applying the most accurate form (Level III of Approximation), which permitted the calculation of ε_x (see Appendix A) and directly calculated the corresponding inclination of the compression stresses (θ). Level III of Approximation was based directly on the equations of the Modified Compression Field Theory (MCFT) [23]. The HCS with fibers were calculated by applying the formula proposed in MC2010 (see Table 6), which included the effect of fibers inside the concrete matrix contribution.

To obtain real predictable resistance concrete, the partial safety factors for material properties were considered in the calculation as γ_c=1 and γ_s=1 (Tables 5 to 7). Moreover, average values were utilized instead of characteristic values present in the formulas.

Code formulae included limitations on several parameters, such as the ρ_l reinforcement ratio for longitudinal reinforcement, the ξ factor which bears in mind size effect, the σ_{ck} average stress acting on the concrete cross-section for an axial force due to prestressing actions, and the minimum concrete contribution due to shear V_{cu} , as presented in Appendix B. None of these limitations affected the values calculated in the beams tested for this paper.

The safety margins (SM= V_{test} / V_{theo}) were used as a reference parameter to compare the results obtained from the different beams and Codes.

Table 7 offers the shear values (experimental and theoretical) and their SM; it also indicates the shear values corresponding to the flexure failure mode and their corresponding SM. An ultimate flexural moment was calculated by taking into account the fibers contribution, according to MC2010. In the SM columns (Table 7), the values exceeding the unit are shown in boldface.

4.3.1 Series I: Shear values according to current Design Codes.

By way of general conclusion, and as expected, all the slabs in Series I presented a failure mode through shear-flexure, therefore theoretical shear values were calculated in regions cracked in bending.

Figure 12 plots the SM of all the HCS in Series I, except HCS (I-50-3.1), which had a failure through bonding. We can observe that the shear SM and the flexure SM are higher than the unit. These results demonstrate that exceeding both shear and flexural theoretical strengths at the same time is possible. However, three HCS (I-50-3.0a, I-50-3.0b and I-50-3.1c) achieved higher SM in the shear than the other

HCS, and this was due to the lower a/d value. We can also note how the MC2010 provisions are better balanced than those from EN1168+RILEM in terms of the elements made with or without fibers. EN1168+RILEM are less conservative than MC2010 when fibers are present.

4.3.2 Series II: Shear values according to current Design Codes.

Figure 13 plots the shear and flexure SM for the tested Series II HCS, assuming regions cracked in bending for EN1168. As with Series I, MC2010 was better balanced than EN1168 when comparing the elements with or without fibers for the same a/d. In any case, the results are very similar for both Code provisions.

Nevertheless, a clear sensitivity to the a/d ratio was detected. Shear SM were greater for the HCS with a low a/d, and obtained values close to 2. On the other hand, shear strength values were more balanced when a/d ratio was higher (3.4). Only HCS II-50-3.4b shows a shear SM lower than 1; it may be justified by a bad surface finishing.

Evidently when flexural failure was observed (II-0-8.6, II-50-8.6, II-70-8.6), failure loads did not reach the theoretical shear strength (*see green boxes in Fig.13*).

In Figure 14, only HCS with web shear tension failures have been represented, plotting together the SM values calculated with both hypotheses: regions cracked in bending (as were plotted in Figure 13) and regions uncracked in bending (Table 5), which means pure shear tension failures. As can be seen in Figure 14, for all HCS, except the II-50-3.4b (because of bad surface finishing), more adjusted SM were obtained assuming uncracked region.

Precracking HCS before shear testing them implied an increase in bearing load that was equal to 24.92%, 31.62% and 21.60% for HCS made with 0 kg/m^3, 50 kg/m^3 and 70 kg/m^3 of fibers, respectively. Figure 15 shows this tendency.

It is evident that flexural precracking not only does not accelerate HCS failure, but makes diagonal tension crack propagation difficult and improves HCS behavior, observing that precracked HCS reached higher ultimate loads than their analogous non precracked (Table 7).

From this Series, we can observe that the Codes are more conservative for the HCS without fibers following the criterion that better adjusts provisions in ductile members [24, 25] because the elements reinforced with fibers display a more ductile behavior than those without fibers. This fact, which the present work detects, agrees with the observations made by Peaston et al. [14].

If the SM in flexure (that is, a capacity achieved in flexure at the time of failure) are represented against the a/d ratio (Figure 16), then the points corresponding to the fiber-reinforced concrete HCS (Series II), which presented a shear tension failure, are over Kani's valley [26]. If the points from FRC elements from Series I (shear compression failure) are observed, then is clear that flexural capacity is also greater than that expected according to Kani's valley. Neither the elements that failed by flexure nor any FRC elements failing in shear show the same tendency.

These results agree with Imam [27], who suggested that the region of diagonal failure disappears completely in Kani's valley when increasing fiber amount and efficiency.

In this way, use of fibers is a possible solution to overcome shear failure since fibers are capable of increasing element strength to its full flexural capacity.

5. Conclusions

According to the tests, the following conclusions can be drawn:

-It is possible to produce fiber-reinforced concrete hollow core slabs (HCS) without encountering technical problems.

-An extensive experimental program has been developed to analyze the shear strength and failure behavior of HCS with different failure modes. The effect of fiber amount and shear span on behavior has been analyzed.

-HCS with fibers reached higher shear capacities than those without fiber reinforcement, and obtain a more ductile behavior. This is a key advantage given the impossibility of placing transverse reinforcements on slabs.

-A clear influence of the a/d ratio on shear strength and on shear behavior has also been detected.

-Model Code 2010 and European standard EN1168+A2 approaches were used to evaluate the HCS shear capacity for both traditional and FRC elements assuming regions cracked in bending. In the EN1168 approach, the fibers effect was introduced as proposed by RILEM. Codes provisions are very similar and are very conservative when the HCS made with FRC shear strength are calculated for loads applied with low a/d and brittle failures caused by web shear tension failure (S). However, they are well adjusted for high a/d ratio values and ductile failures caused by flexure (F) or shear-flexure (SF).

-The model proposed in EN1168 to evaluate the shear capacity in regions uncracked in bending was the most adjusted for HCS with web shear tension failures (S).

-The HCS which were previously precracked in flexure show improved shear behavior, and obtain higher safety margins (20-30%) than not precracked HCS.

-Use of fibers is a possible solution to overcome shear failure since fibers are capable of increasing element strength to its full flexural capacity, thus attenuating Kani's valley.

Acknowledgments

The authors of this work wish to thank the research bureau of the Spanish Ministry of Science and Innovation and the Plan E, for the funding of the project "BIA 2009-12722" . The collaboration of the precast industry "PREVALESA S.L" is also acknowledged.

References

[1] Hawkins N M, Ghosh S K. Shear Strength of Hollow-Core Slabs. PCI Journal 2006; pp.110-114.

[2] Yang L. Design of prestressed hollow core slabs with reference to web shear failure. Journal of Structural Engineering ASCE 1994; 120 (9):2675-2696.

[3] Girhammar U A. Design principles for simply supported prestressed hollow core slabs. Structural Engineering Review 1992; 4 (4): 301-316.

[4] Walraven J C, Mercx W P M. The bearing capacity of prestressed hollow core slabs. Heron 1983; 28 (3).

[5] Becker R J, Buettner D R. Shear Tests of Extruded Hollow-Core Slabs. Precast/Prestressed Concrete Institute Journal, 1985; 30 (2): 40-54.

[6] Pisanty A, Regan P E. Direct assessment of the tensile strength of the web in prestressed precast hollow-core slabs. Materials and Structures 1991; 24: 451-455.

[7] Pisanty A. The shear strength of extruded hollow-core slabs. Materials and Structures 1992; 25: 224-230.

[8] Paine K A. Trial Production of Fibre Reinforced Hollow Core Slab. Research Report SR96007, 1996, 38 pp.

[9] Paine K A. Steel fibre reinforced concrete for prestressed hollow core slabs, 1998, PhD thesis, University of Nottingham, pp. 325.

[10] Elliott K S, Peaston C H, Paine K A. Experimental and theoretical investigation of the shear resistance of steel fibre reinforced prestressed concrete X-beams-Part I: Experimental work. Materials and Structures 2002; 35: 519-527.

[11] Elliott K S, Peaston C H, Paine K A. Experimental and theoretical investigation of the shear resistance of steel fibre reinforced prestressed concrete X-beams-Part II: Theoretical analysis and comparison with experiments. Materials and Structures 2002; 35: 528-535.

[12] Bertagnoli G, Mancini G. Failure analysis of hollow-core slabs tested in shear. Structural Concrete (fib Journal) 2009; 10 (3):139-152.

[13] Araujo C, Loriggio D, Da Camara J. Anchorage failure and shear design of hollow-core slabs. Structural Concrete 2011; 12 (2): 109-119.

[14] Peaston C, Elliott K, Paine K. Steel Fiber Reinforcement for Extruded Prestressed Hollow Core Slabs. ACI Special Publication 1999; 182: 87-107.

[15] Cuenca E, Serna P, Pelufo M.J. Structural behavior of self-compacting and fiber reinforced concrete under shear loading. Proceedings of the International Association for Shell and Spatial Structures (IASS) Symposium 28 September -2 October 2009, Valencia Spain.

[16] Cuenca E, Serna P. Shear behavior and Mode of Failures analysis of different structural elements made with fiber reinforced concrete. 8th fib PhD Symposium in Kgs. Lyngby, Denmark June 20-23 2010.

[17] Cuenca E, Serna P. Shear behavior of self-compacting concrete and fiber reinforced concrete beams. 6th International RILEM Symposium on Self-Compacting Concrete SCC2010, Montreal, Canada 2010.

[18] UNE-EN 1168+A2. Precast concrete products. Hollow core slabs, 2006.

[19] *fib* bulletin 55. Model Code 2010 – First complete draft, 2010; Vol.1, 318 pp.

[20] *fib* bulletin 56. Model Code 2010 – First complete draft, 2010; Vol.2, 312 pp.

[21] RILEM. RILEM TC 162-TDF: Test and design methods for steel fibre reinforced concrete, σ-ε-Design method. Final Recommendation. RILEM 2003; 36:560-567.

[22] European Committee for Standardization. Eurocode 2:Design of Concrete Structures – EN 1992-1-1, 2004.

[23] Vecchio F, Collins M. The Modified compression Field Theory for reinforced concrete elements subjected to shear. ACI Journal 1986; 83(2):219-231.

[24] Cladera A, Marí A. Shear design of reinforced and prestressed concrete beams: a proposal for code procedure. Hormigón y Acero 2006; 242 (4):51-63.

[25] Cladera A, Marí A. Shear design procedure for reinforced normal and high-strength concrete beams using artificial neural networks. Part II: beams with stirrups. Engineering Structures 2004; 26:927-936.

[26] Kani G N J. The Riddle of Shear Failure and its solution. ACI Journal 1964; 61 (4):441-467.

[27] Imam M, Vandewalle L, Mortelmans F and Van Gemert D. Shear domain of fibre-reinforced high-strength concrete beams. Engineering Structures 1997; 19 (9):738-747.

FIGURE CAPTIONS

Fig.1. Cross-section of HCS. Dimensions in millimeters

Fig. 2. Extrusion process

Fig. 3. How the surface of HCS looked

Fig.4. Loads and supports distribution on HCS

Fig.5. Test set-up. Shear diagonal tension failure

Fig.6. Section took in consideration in web shear tension failure calculations.

Fig. 7. Shear-flexure failure

Fig. 8. Flexure failure

Fig. 9. Anchorage failure of strands

Fig. 9-a. Sliding of the strands in concrete

Fig. 9-b. Crack caused by anchorage failure

Fig. 10. Load-deflection response (Series I)

Fig. 11. Load-deflection response (Series II)

Fig. 11-a. HCS with 0kg/m^3 of fibers

Fig. 11-b. HCS with 50kg/m^3 of fibers

Fig. 11-c. HCS with 70kg/m^3 of fibers

Fig. 11-d. HCS with a/d=3.4

Fig. 12. Shear safety margins (Series I)

Fig. 13. Shear safety margins (Series II)

Fig. 14. Shear safety margins of HCS with web shear tension failure (Series II).

Fig. 15. Precrack influence on shear strength for HCS with a/d=3.4

Fig. 16. Own database inside Kani's valley

Table 1
Reinforcement characteristics

Series	*Slab*	*Initial tensile [MPa]*	*Prestressed losses (%)*	r_{inf} *(mm)*	*REINFORCEMENT POSITION*					ρ_l *(%)*	σ_c *(MPa)*
					U	**U'**	**V**	**X**	**Z**		
I	PF26.20	1255	19.7	30	2ϕ5	5ϕ9.3	--	--	4ϕ5	0.5	2.87
II	PF26.16	1255	27.2	25	25ϕ5	--	9ϕ5	4ϕ5	4ϕ5	1	5.69

Table 2
Mix design of the HCS tested.

(kg/m^3)	***TC***	***FRC-50***	***FRC-70***
Coarse aggregate (6/10mm)		843	
Sand (0/4mm)		690	
Sand (0/6mm)		311	
Cement		411	
Water (liters)		198	
W/C ratio		0.48	
Fibers	0	50	70
Superplasticizer (liters)	1.5	1.5	1.6
Admixture for extruded concretes (l)	0.8	0.8	0.7
Mixing time (min)	1.5	4.3	5.4

Table 3
Concrete mechanical properties. Average values.

Series	*Concrete*	f_c *[MPa]*	f_{R1} *[MPa]*	f_{R2} *[MPa]*	f_{R3} *[MPa]*	f_{R4} *[MPa]*
I (PF 26.20)	*TC*	54.2	--	--	--	--
	FRC-50	50.4	2.75	2.85	2.83	2.66
II (PF 26.16)	*TC*	43.8	--	--	--	--
	FRC-50	38.2	4.25	4.66	4.70	4.37
	FRC-70	35.9	5.74	6.03	5.80	5.47

Table 4
Shear tests description and Specimen ID to each HCS

Series	*HCS*	*Specimen ID*	*Fibers amount (kg/m^3)*	*a/d ratio*	*Cantilever span (mm)**	l_{pt} *(mm)*	l_{crit} *(mm)*	V_{test} *(kN)*	*Failure Mode*
I	1	I-0-4.1	0	4.1	600	400.20	785.66	131.15	SF
	2	I-0-4.3a		4.3	630		815.66	131.11	SF
	3	I-0-4.3b		4.3	630		815.66	134.90	SF
	4	I-50-3.1	50	3.1	120	420.07	305.66	160.19	A
	5	I-50-3.9a		3.9	700		885.66	162.10	SF
	6	I-50-3.9b		3.9	700		885.66	162.10	SF
	7	I-50-4.3		4.3	860		1045.66	152.61	SF
	8	I-50-4.4		4.4	870		1055.66	158.62	SF
	9	I-50-3.0a		3.0	120		305.66	172.95	SF
	10	I-50-3.0b		3.0	2120		2305.66	200.63	SF
	11	I-50-3.1c		3.1	2035		2220.66	189.43	SF
II	12	II-0-2.3	0	2.3	210	350.62	395.66	310.80	A
	13	II-0-3.4		3.4	270		455.66	213.10	S
	14	II-0-3.4 (P)		3.4	2105		2290.66	266.20	S
	15	II-0-8.6		8.6	250		435.66	131.60	SF
	16	II-50-2.3	50	2.3	500	384.10	685.66	410.00	S
	17	II-50-3.4a		3.4	225		410.66	236.70	S
	18	II-50-3.4 (P)		3.4	260		445.66	288.70	S
	19	II-50-3.4b		3.4	2500		2685.66	202.00	S
	20	II-50-8.6		8.6	270		455.66	146.10	F
	21	II-70-2.3a	70	2.3	225	400.33	410.66	310.70	S
	22	II-70-2.3b		2.3	215		400.66	310.70	A
	23	II-70-3.4a		3.4	250		435.66	266.70	S
	24	II-70-3.4 (P)		3.4	290		475.66	315.00	S
	25	II-70-3.4b		3.4	290		475.66	251.40	S
	26	II-70-8.6		8.6	230		415.66	135.20	F

*SF: Shear-flexure failure; S: Web shear tension failure; F: flexure failure; A: Anchorage failure of strands. (P)=Hollow core slab precracked in flexure; *Values correspond to the cantilever span nearest the failure side; l_{pt}: basic value of the transmission length; l_{crit}: distance between the end of the slab and the critical section.*

Table 5
Shear resistance (kN) of the regions uncracked in bending according to EN 1168+A2 and RILEM

HCS	*Specimen ID*	V_{test}	*Failure Mode*	V_{Rdc} *(EN1168+A2)*	V_f *RILEM*	V_{theo}, *uncracked in bending*	*SM (V)*
12	II-0-2.3	310.80	A	191.58	0.00	191.58	**1.62**
13	II-0-3.4	213.10	S	207.30	0.00	207.30	**1.03**
16	II-50-2.3	410.00	S	230.04	78.77	308.81	**1.33**
17	II-50-3.4a	236.70	S	170.22	78.77	248.99	0.95
19	II-50-3.4b	202.00	S	258.44	78.77	337.21	0.60
21	II-70-2.3a	310.70	S	159.29	98.83	258.12	**1.20**
22	II-70-2.3b	310.70	A	156.75	98.83	255.58	**1.22**
23	II-70-3.4a	266.70	S	165.45	98.83	264.28	**1.01**
25	II-70-3.4b	251.40	S	174.87	98.83	273.70	0.92

Table 6
Current Codes shear formulas for elements without stirrups for regions cracked in bending.

Code	**Theoretical Shear (V)**	
	Concrete contribution V_{cu} **Fibers contribution V_{fu}**	
EN 1168+A2 [18] + RILEM [21]	$V_{cu} = [(0.18/\gamma_c)\cdot\xi\cdot(100\cdot\rho_l\cdot C_2)^{1/3} + 0.15\cdot\sigma_{ck}]\cdot b_o\cdot d$ $V_{fu} = k_f\cdot 0.7\cdot\xi\cdot 0.18\cdot(f_{R4k}/\gamma_c)\cdot b_o\cdot d$	$C_2 = f_{cv}$
MC2010 [19, 20] Without fibers:	$V_{cu} = k_v\cdot(\sqrt{f_{ck}}/\gamma_c)\cdot z\cdot b_o$ *(Level III Approximation)*	----------
MC2010 [19, 20] With fibers:	$V_{cu} + V_{fu} = [(0.18/\gamma_c)\cdot\xi\cdot(100\cdot\rho_l\cdot C_2)^{1/3} + 0.15\cdot\sigma_{ck}]\cdot b_o\cdot d$ $C_2 = (1+7.5\cdot(f_{Ftuk}/f_{ctk}))\cdot f_{ck}$	

Table 7
Shear values (kN) calculated without safety factors using current Design Codes
(average values for mechanical properties: compression and residual flexural strength).

HCS	*Specimen ID*	V_{test}	*Failure Mode*	$V_{FLEXURE}$	*SM (F)*	$V_{EN1168+RILEM}$	*SM (V)* $_{EN1168+RILEM}$	V_{MC2010}	*SM (V)* $_{MC2010}$
1	I-0-4.1	131.15	SF	133.86	0.98	100.55	**1.30**	104.16	**1.26**
2	I-0-4.3a	131.11	SF	126.63	**1.04**	102.25	**1.28**	101.80	**1.29**
3	I-0-4.3b	134.90	SF	125.21	**1.08**	102.25	**1.32**	101.31	**1.33**
4	I-50-3.1	160.19	A	196.42	0.82	149.18	**1.07**	128.10	**1.25**
5	I-50-3.9a	162.10	SF	153.86	**1.05**	149.18	**1.09**	128.10	**1.27**
6	I-50-3.9b	162.10	SF	153.86	**1.05**	149.18	**1.09**	128.10	**1.27**
7	I-50-4.3	152.61	SF	139.87	**1.09**	149.18	**1.02**	128.10	**1.19**
8	I-50-4.4	158.62	SF	137.79	**1.15**	149.18	**1.06**	128.10	**1.24**
9	I-50-3.0a	172.95	SF	199.25	0.87	149.18	**1.16**	128.10	**1.35**
10	I-50-3.0b	200.63	SF	197.82	**1.01**	149.18	**1.34**	128.10	**1.57**
11	I-50-3.1c	189.43	SF	197.12	0.96	149.18	**1.27**	128.10	**1.48**
12	II-0-2.3	310.80	A	560.58	0.55	150.10	**2.07**	182.42	**1.70**
13	II-0-3.4	213.10	S	373.72	0.57	150.10	**1.42**	182.42	**1.17**
14	II-0-3.4 (P)	266.20	S	373.72	0.71	150.10	**1.77**	182.42	**1.46**
15	II-0-8.6	131.60	SF	149.49	0.88	150.10	0.88	115.25	**1.14**
16	II-50-2.3	410.00	S	546.11	0.75	224.62	**1.83**	200.81	**2.04**
17	II-50-3.4a	236.70	S	364.07	0.65	224.62	**1.05**	200.81	**1.18**
18	II-50-3.4 (P)	288.70	S	364.07	0.79	224.62	**1.29**	200.81	**1.44**
19	II-50-3.4b	202.00	S	364.07	0.55	224.62	0.90	200.81	**1.01**
20	II-50-8.6	146.10	F	144.13	**1.01**	224.62	0.65	200.81	0.73
21	II-70-2.3a	310.70	S	540.50	0.57	243.15	**1.28**	207.60	**1.50**
22	II-70-2.3b	310.70	A	540.50	0.57	243.15	**1.28**	207.60	**1.50**
23	II-70-3.4a	266.70	S	360.34	0.74	243.15	**1.10**	207.60	**1.28**
24	II-70-3.4 (P)	315.00	S	360.34	0.87	243.15	**1.30**	207.60	**1.52**
25	II-70-3.4b	251.40	S	360.34	0.70	243.15	**1.03**	207.60	**1.21**
26	II-70-8.6	135.20	F	144.13	0.94	243.15	0.56	207.60	0.65

*P=Hollow core slab precracked in flexure; *Bond failure.*
Failures: SF: Shear-flexure failure; S: Web shear tension failure; F: flexure failure; A: Anchorage failure of strands.

Appendix A. Notation

A_p	Cross-sectional area of prestressed reinforcement
A_s	Cross-sectional area of longitudinal tension reinforcement
b_f	flange width
b_o	web width
d	effective depth
f_{ctk}	characteristic value of the tensile strength for the concrete matrix
f_{Ftuk}	characteristic ultimate residual tensile strength value for fiber-reinforced concrete
f_{p0}	stress in strands when the strain in the surrounding concrete is zero
f_{R3k}	residual flexural tensile strength corresponding to CMOD=2.5mm (according to EN 14645)
f_{R4k}	residual flexural tensile strength corresponding to CMOD=3.5mm (according to EN 14645)
$f_{y\alpha,k}$	yielding strength of shear reinforcement steel
I	second moment of area
k_f	factor to take into account the flanges contribution in the T-sections (RILEM)
l_{pt2}	upper bound value of the transmission length of the prestressing element: $l_{pt2}=1.2 \cdot l_{pt}$
l_x	distance of section considered from starting point of the transmission length
S	first moment of area above and about the centroidal axis
V_{cu}	design shear resistance attributed to concrete
V_{fu}	design shear resistance attributed to fibers
V_{u2}	design shear resistance
z	internal lever arm corresponding to the maximum bending time. In the shear analysis, an approximate value of z=0.9·d can normally be used.
α_l	$=l_x/l_{pt2} \leq 1$ for pretensioned tendons
β	reduction factor referred to the transmission length (β=0.9)
γ_c	partial safety factor for concrete material properties
γ_s	partial safety factor for the material properties of reinforcement and prestressing steel
ε_x	longitudinal strain at the element's mid-depth
θ	inclination of compression stresses
ξ	factor that takes into account size effect
ρ_l	reinforcement ratio for longitudinal reinforcement
σ_{ck}	average stress acting on the concrete cross-section for an axial force due to prestressing actions
φ	reduction factor (φ=0.8)

Appendix B. Parameters determination and their limitations

Common limitations for all Codes:

$\xi = 1+\sqrt{(200/d)} \leq 2.0$ (B.1)

$\rho_l = (A_s+A_p)/(b_o \cdot d) \leq 0.02$ (B.2)

Particular limitations of each Code:

$\sigma_{ck}=[(N_k+P_k)/(b_o \cdot d)]<0.2 \cdot f_{ck}$ (EC2 and MC2010 for FRC) (B.3)

$k_f = 1+n \cdot (h_f/b_o) \cdot (h_f/d) < 1.5$ (RILEM) (B.4)

$n=[(b_f-b_o)/h_f]<3$ and $n<(3 \cdot b_o/h_f)$ (RILEM) (B.5)

$V_{cu,\,min} = [0.035 \cdot \xi^{3/2} \cdot f_{cv}^{1/2} + 0.15 \cdot \sigma_{ck}] \cdot b_o \cdot d$ (EC2 and MC2010 for FRC) (B.6)

Parameters influencing V_{cu} (MC2010):

$\theta = 29^o + 7000 \cdot \varepsilon_x$ (B.7)

$\varepsilon_x=[M_{Ed}/z + V_{Ed} + 0.5 \cdot N_{Ed} - A_p \cdot f_{p0}] / [2 \cdot (E_s \cdot A_s + E_p \cdot A_p)]$ (B.8)

$k_v=0.4 \cdot 1300 / [(1 +1500 \cdot \varepsilon_x) \cdot (1000 + 0.7 \cdot k_{dg} \cdot z)]$ if $\rho_w=0$ (B.9)

$k_v=0.4 / (1 +1500 \cdot \varepsilon_x)$ if $\rho_w \geq 0.08 \cdot \sqrt{f_{ck}} / f_{yk}$ (B.10)

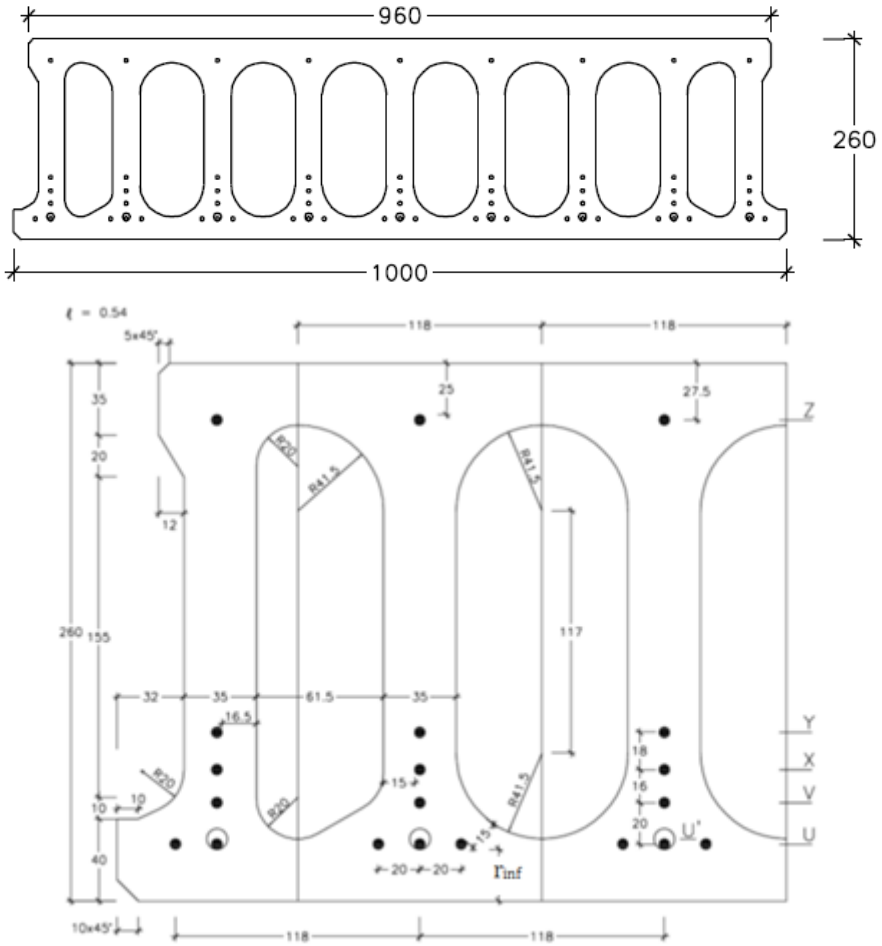

Fig.1. Cross-section of HCS. Dimensions in millimeters

Fig. 2. Extrusion process

Fig. 3. How the surface of HCS looked

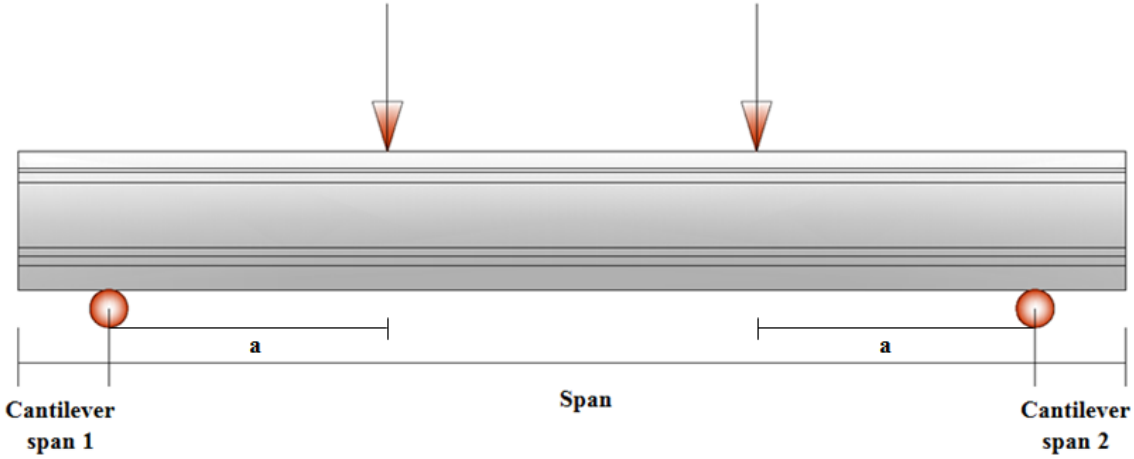

Fig.4. Loads and supports distribution on HCS

Fig.5. Test set-up. Shear diagonal tension failure

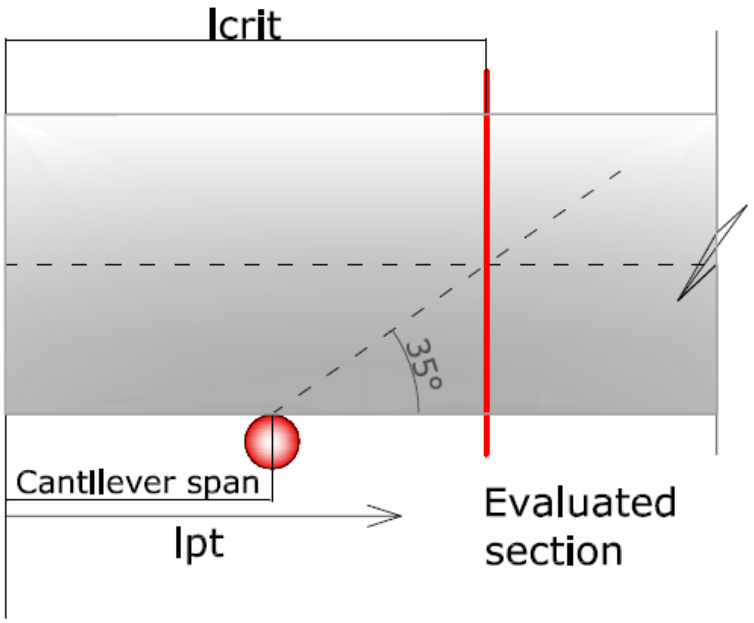

Fig.6. Section took in consideration in web shear tension failure calculations.

Fig. 7. Shear-flexure failure.

Fig. 8. Flexure failure.

Fig. 9a. Sliding of the strands in concrete **Fig. 9b.** Crack caused by anchorage failure

Fig. 9. Anchorage failure of strands

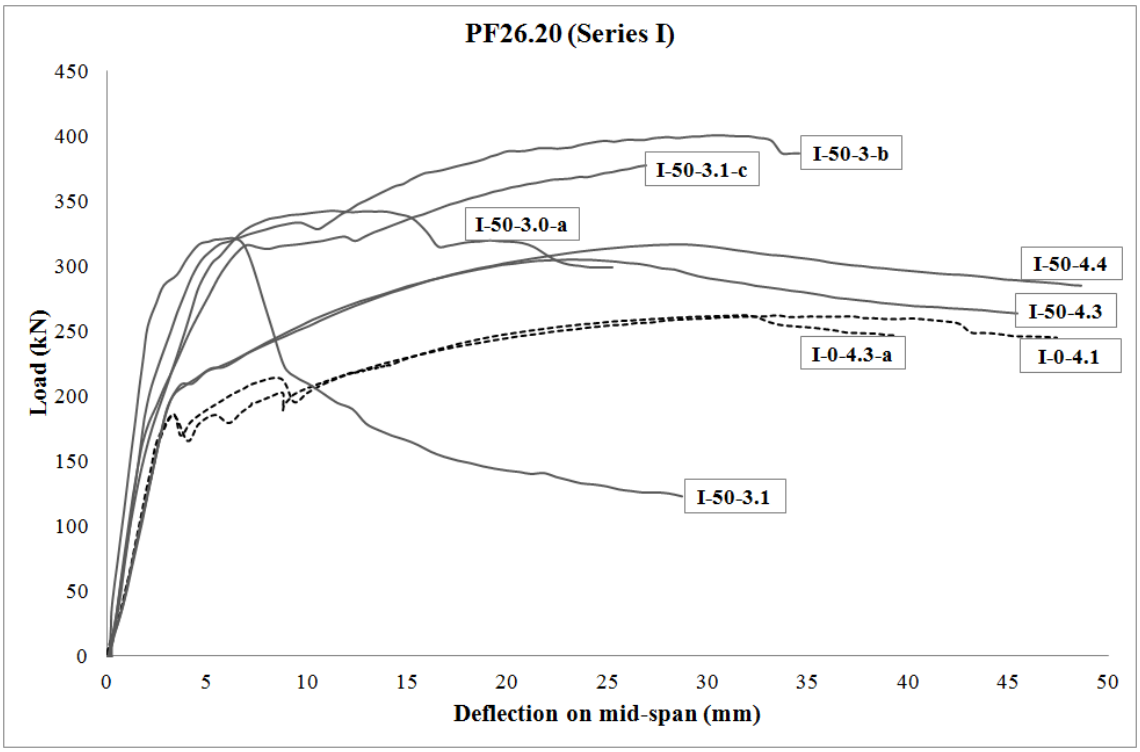

Fig. 10. Load-deflection response (Series I).

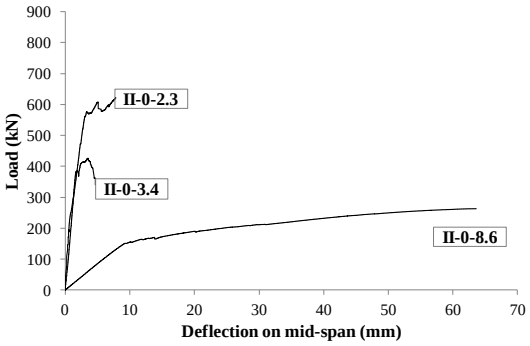

Fig. 11-a. HCS with 0kg/m^3 of fibers

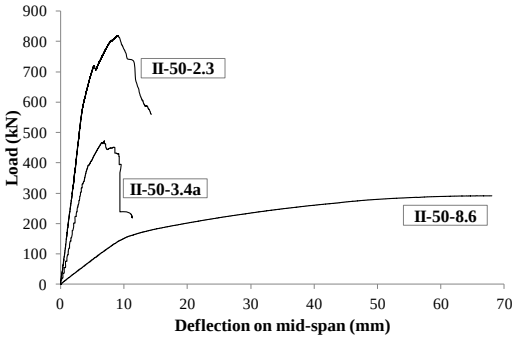

Fig. 11-b. HCS with 50kg/m^3 of fibers

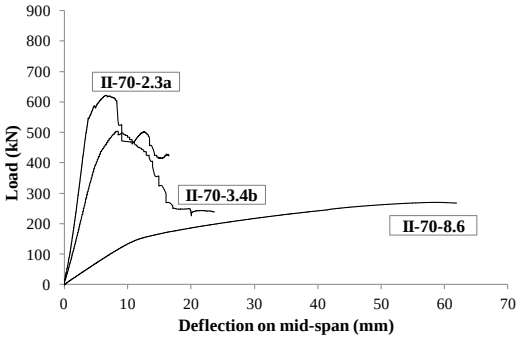

Fig. 11-c. HCS with 70kg/m^3 of fibers

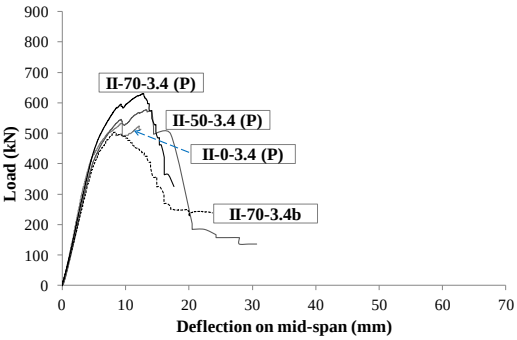

Fig. 11-d. HCS with a/d=3.4

Fig. 11. Load-deflection response (Series II).

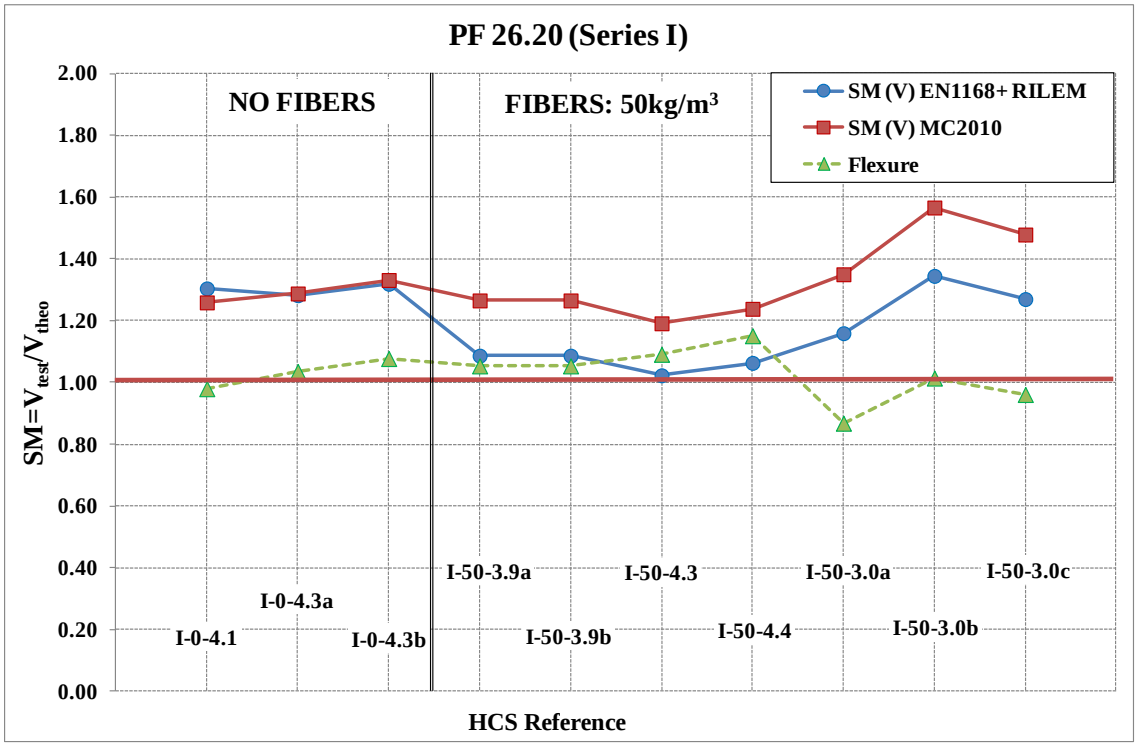

Fig. 12. Shear safety margins (Series I).

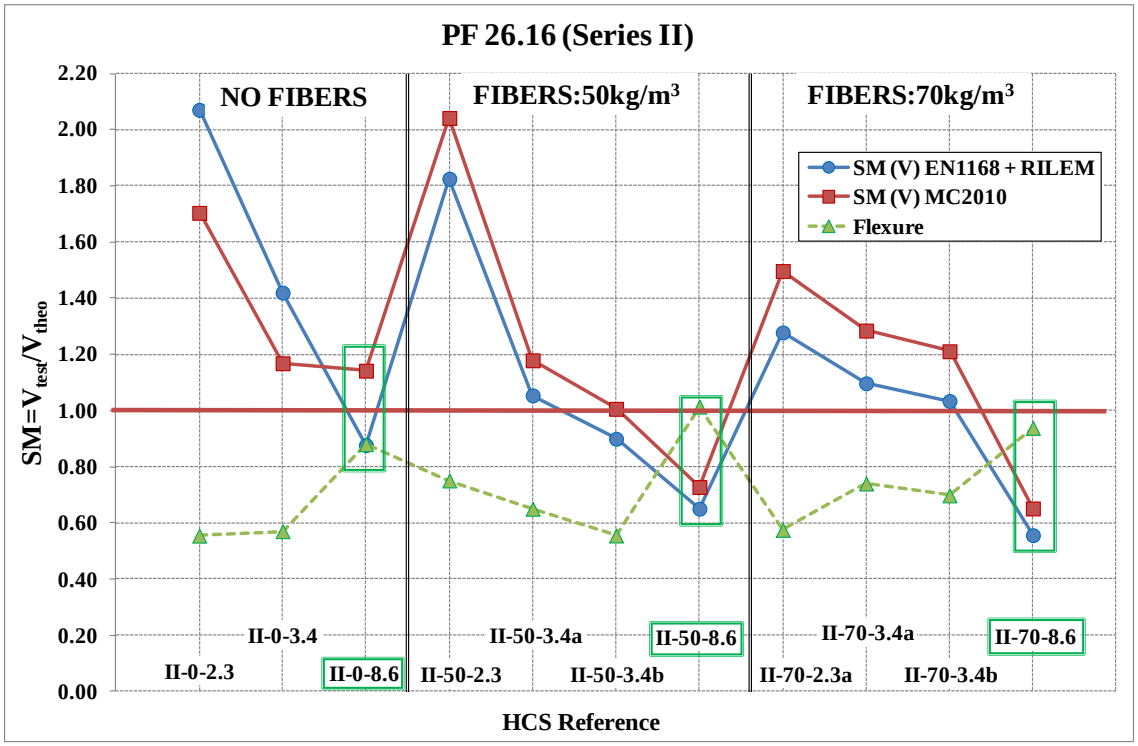

Fig. 13. Shear safety margins assuming regions cracked in bending (Series II).

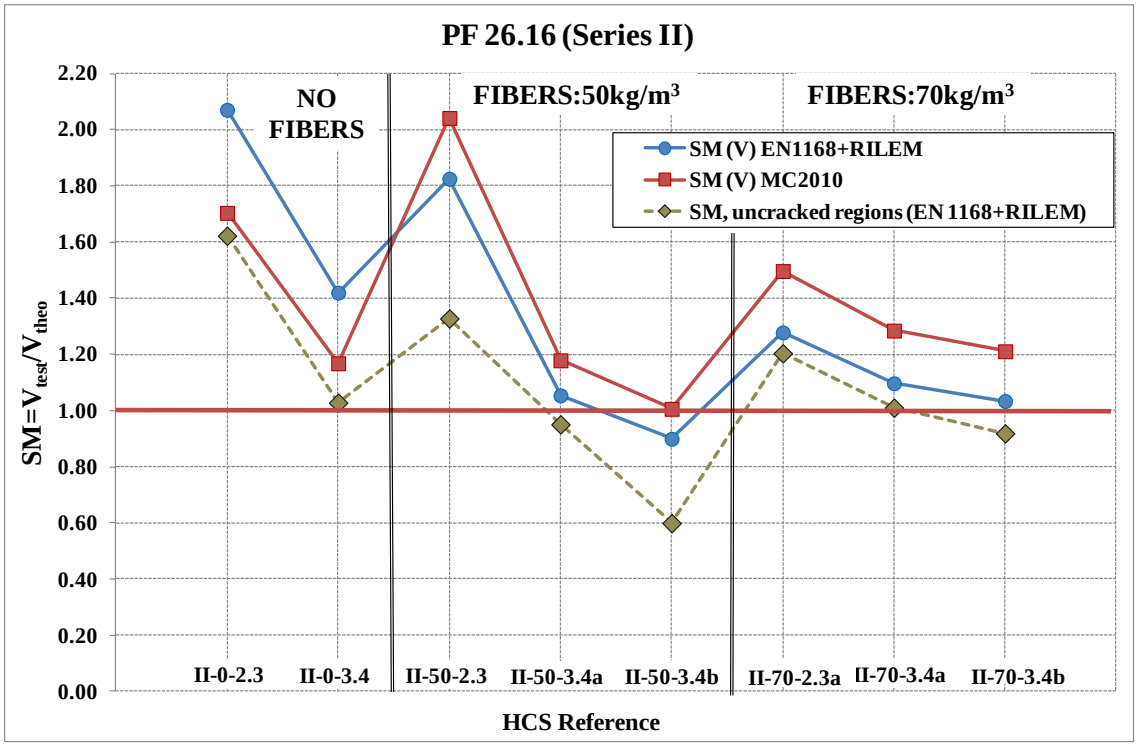

Fig. 14. Shear safety margins of HCS with web shear tension failure (Series II).

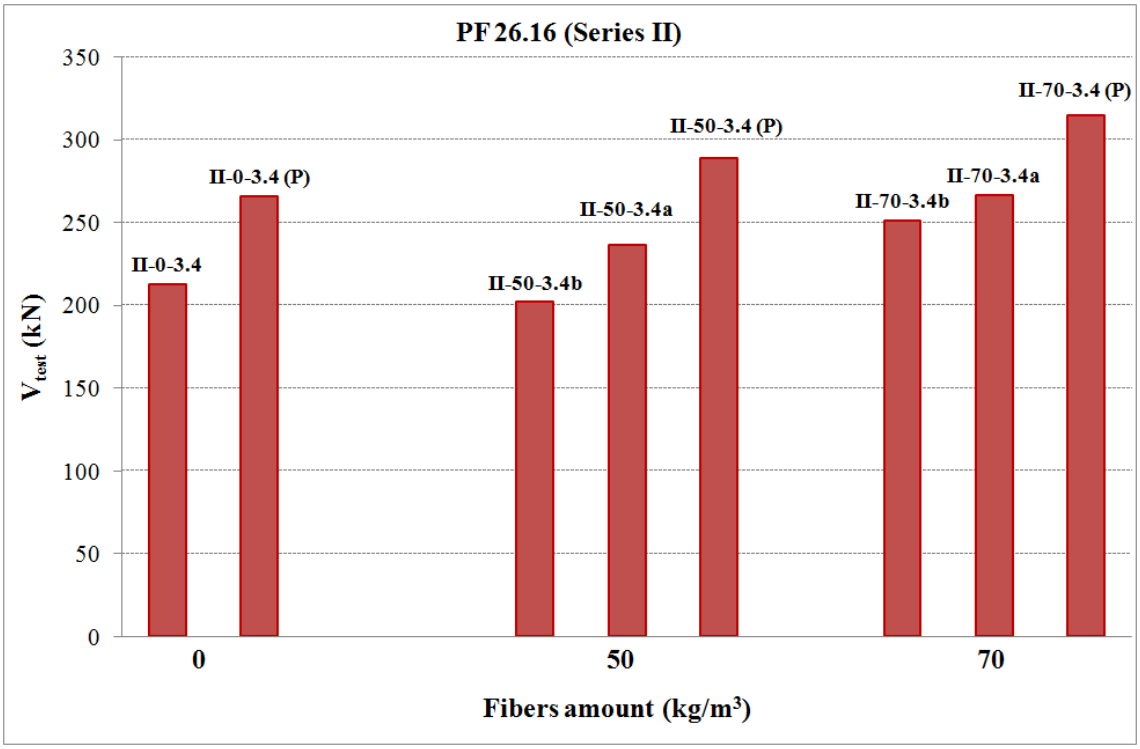

Fig. 15. Precrack influence on shear strength for HCS with a/d=3.4

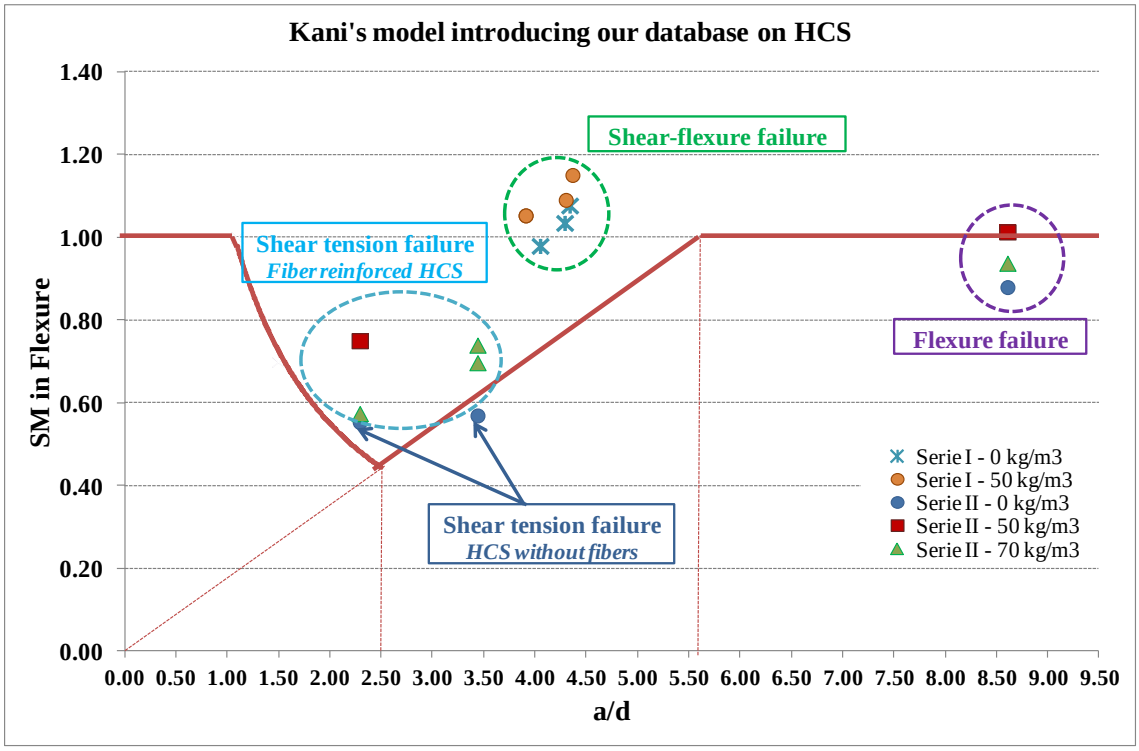

Fig. 16. Own database inside Kani's valley